AD-A259 605

NASA Contractor Report 189734
ICASE Report No. 92–63

ICASE

VORTEX BREAKDOWN INCIPIENCE: THEORETICAL CONSIDERATIONS

S. A. Berger
G. Erlebacher

DTIC
ELECTE
JAN26 1993
S E D

NASA Contract Nos. NAS1–18605 and NAS1–19480
November 1992

Institute for Computer Applications in Science and Engineering
NASA Langley Research Center
Hampton, Virginia 23681–0001

Operated by the Universities Space Research Association

93-01346

National Aeronautics and Space Administration
Langley Research Center
Hampton, Virginia 23665-5225

DISTRIBUTION STATEMENT A
Approved for public release;
Distribution Unlimited

98 1 25 096

Accesion For
NTIS CRA&I
DTIC TAB
Unannounced
Justification
By
Distribution /
Availability Codes
Dist | Avail and / or Special
A-1

VORTEX BREAKDOWN INCIPIENCE: THEORETICAL CONSIDERATIONS

S. A. Berger[1]
University of California
Berkeley, CA 94720

G. Erlebacher[1]
Institute for Computer Applications in Science and Engineering
NASA Langley Research Center
Hampton, VA 23681-0001

DTIC QUALITY INSPECTED 5

ABSTRACT

The sensitivity of the onset and the location of vortex breakdowns in concentrated vortex cores, and the pronounced tendency of the breakdowns to migrate upstream have been characteristic observations of experimental investigations; they have also been features of numerical simulations and led to questions about the validity of these simulations. This behavior seems to be inconsistent with the strong time-like axial evolution of the flow, as expressed explicitly, for example, by the quasi-cylindrical approximate equations for this flow. An order-of-magnitude analysis of the equations of motion near breakdown leads to a modified set of governing equations, analysis of which demonstrates that the interplay between radial inertial, pressure, and viscous forces gives an elliptic character to these concentrated swirling flows. Analytical, asymptotic, and numerical solutions of a simplified non-linear equation are presented; these qualitatively exhibit the features of vortex onset and location noted above.

[1]This research was supported by the National Aeronautics and Space Administration under NASA Contract Nos. NAS1-18605 and NAS1-19480 while the authors were in residence at the Institute for Computer Applications in Science and Engineering (ICASE), NASA Langley Research Center, Hampton, VA 23681-0001.

1. Introduction

The study of the breakdown of the cores of strong longitudinal vortices has been of recurring interest for many years. Breakdown may be described as the abrupt change in the structure of the core of a vortex, often characterized by the presence of a free stagnation point on the axis of the vortex and a corresponding divergence of the stream surfaces near the axis, and in some cases a region of reversed flow. In addition to being of theoretical interest, vortex breakdown has important technological applications, both aerodynamic and non-aerodynamic [1]. In some applications vortex breakdown is beneficial, for example, in leading to enhanced mixing or momentum or heat exchange; or destructive, as in degradation of aerodynamic performance. Vortex breakdown may play an important role in vortex dynamics in general, and perhaps also in transition to turbulence. Given the importance of vortex breakdown, it is quite remarkable that the basic underlying mechanism leading to breakdown is not yet known or generally accepted! This is not for lack of postulated explanations the literature abounds with them. More remarkable yet is that these explanations are so vastly different in what they postulate to be the underlying mechanism; these, variously, affirm (their principal claimants indicated parenthetically) that:

(i) vortex breakdown is similar to the separation of a two-dimensional boundary layer (Hall [2,3], Mager [4]);

(ii) vortex breakdown is a consequence of hydrodynamic instability (Ludwieg [5,6]);

(iii) vortex breakdown is dependent on the existence of a critical state, and is a finite transition between states, analogous to a hydraulic jump (Squire [7], Benjamin [8,9]);

(iv) vortex breakdown is like a solitary wave, or soliton, the result of the trapping of long, weakly nonlinear waves propagating in nearly critical swirling flows (Leibovich [10,11]).

To a greater or lesser degree each of these theories fails to explain fully, or adequately, breakdown in all its aspects. Experiments and numerical simulations have failed to resolve the matter satisfactorily. How can one account for this failure? A number of reasons present themselves. First, experiments and measurements are difficult. There is a tendency for the breakdown to migrate back and forth in the test section or on the aerodynamic surface. Measurements, whether invasive (e.g. hot wires) or non-invasive (e.g. LDV), and flow visualization are difficult to obtain and to interpret in these potentially unsteady, three-dimensional flows. Over the years some of the seemingly different postulated physical mechanisms of vortex breakdown have been shown to be equivalent or related, leading to the same or similar criteria for breakdown. To the extent that the various theories predict a criterion for

vortex breakdown the predictions are quite similar [12], namely that $tansup - 1$ $v/w \approx 57$ (de or $v/w \approx 1.5$, where v and w are the swirl and axial velocities, respectively, so this cannot be used to distinguish among or between the various physical mechanisms and their corresponding theoretical formulations.

As for numerical simulations of breakdown using the full Navier-Stokes, or inviscid Euler equations, until recently these generally required the assumption of axisymmetry and steadiness of the flow [13-16]. This is not true of the more recent calculations, for example, those by Kuruvila & Salas [17], Spall et al. [18,19], Breuer & Hanel [20], and Menne & Liu [21], all of which solve the unsteady, three-dimensional, fully viscous Navier-Stokes equations (but not all of them are necessarily time-accurate solutions). Common characteristics of many of the earlier and these most recent numerical simulations, and for that matter of the experiments as well, are: (i) extreme sensitivity to flow parameters (such as swirl velocity ratio, external axial velocity variation, or pressure gradient); (ii) suddenness of breakdown (i.e. no evidence of the growth of an instability of the basic swirling flow); and (iii) a tendency for the breakdowns to migrate upstream to the initial station or computational cell. In some simulations [18] this is avoided by specifying the external axial velocity gradient.

This last characteristic of these computations is the case, at least, for unbounded or "open" flows, e.g. aerodynamic flows and flows in diverging channels. Numerically simulated breakdowns, usually in the form of steady axisymmetric bubbles, that occur in bounded or confined swirling flows, for example, in finite closed cylinders with one endwall rotating (Lugt [22,23], Neitzel [24]) or flow in the gap between rotating spheres (Bar-Yoseph et al. [25]) do not exhibit this behavior, nor do experiments on these flows (Escudier [26]). This tendency of the breakdowns to migrate to the initial station has caused questions to be raised about the validity of such numerical simulations [27]. Another potential concern or question in the simulations of breakdown is the appropriate downstream boundary conditions to impose in order to "close" the flow domain, a question whether one uses the elliptic Euler or Navier-Stokes equations. What makes these issues more troubling is the question of the extent to which difficulties with the numerical simulations, including the slow rates of convergence to final steady states often encountered, reflect physical reality, or, in other words, are intrinsic aspects of the onset and location of breakdown.

This paper addresses and attempts to answer one of the above questions: the extreme sensitivity of the breakdown location to certain flow parameters and the pronounced tendency for the breakdown to migrate upstream. The theoretical explanation for these effects is given in Section 2 where the "quasi-cylindrical equations" (Hall [2]) are analyzed in some detail. These equations are simplified forms of the Navier-Stokes equations derived by making boundary layer-like assumptions and approximations, and like those equations are parabolic,

reflecting a strong "time-like" character to the spatial evolution of these thin strongly-swirling vortex cores. We show that near breakdown, in the radial momentum equation, which is a purely inviscid equation in the quasi-cylindrical approximation, the radial viscous diffusion term must be retained. An analysis of this modified set of equations, which would seem, like the original equations, to be parabolic since no axial viscous diffusion terms appear, shows that in fact they have elliptic-like characteristics. This is explicitly shown by demonstrating that the equations may be recast in the form of an elliptic-integro-partial differential equation for the axial velocity variation. In Section 3 a simplified, but still non-linear, equation is employed as a model of the full integro-differential equation and its full solution given. Included in this section is also a matched asymptotic expansion of the equation in the limit of large Reynolds numbers. (This solution yields simpler expressions for the axial velocity variation near breakdown and its explicit dependence on flow and fluid parameters.) This section concludes with an order-of-magnitude analysis which explicitly relates the constant appearing in the simplified equation to the primary flow parameters: the core Reynolds number, the flow divergence, the swirl velocity ratio, and the (non-dimensional) core circulation. In Section 4 explicit results of the exact analytic solution presented in Section 3 for a representative range of values of the flow parameters are presented and discussed.

2. Mathematical Model

We assume the flow is steady, axisymmetric and laminar. The governing Navier-Stokes equations in a cylindrical coordinate system $\overline{r}$, θ, $\overline{z}$, with corresponding velocity components $\overline{u}$, $\overline{v}$, $\overline{w}$ (the overbars denote dimensional variables) are

$$\frac{1}{\overline{r}}\frac{\partial}{\partial \overline{r}}(\overline{r}\,\overline{u}) + \frac{\partial \overline{w}}{\partial \overline{z}} = 0, \tag{2.1}$$

$$\overline{u}\frac{\partial \overline{u}}{\partial \overline{r}} + \overline{w}\frac{\partial \overline{u}}{\partial \overline{z}} - \frac{\overline{v}^2}{\overline{r}} = -\frac{1}{\rho}\frac{\partial \overline{p}}{\partial \overline{r}} + \nu\left[\frac{\partial}{\partial \overline{r}}\left(\frac{1}{\overline{r}}\frac{\partial}{\partial \overline{r}}(\overline{r}\,\overline{u})\right) + \frac{\partial^2 \overline{u}}{\partial \overline{z}^2}\right], \tag{2.2}$$

$$\overline{u}\frac{\partial \overline{v}}{\partial \overline{r}} + \overline{w}\frac{\partial \overline{v}}{\partial \overline{z}} + \frac{\overline{u}\,\overline{v}}{\overline{r}} = \nu\left[\frac{\partial}{\partial \overline{r}}\left(\frac{1}{\overline{r}}\frac{\partial}{\partial \overline{r}}(\overline{r}\,\overline{v})\right) + \frac{\partial^2 \overline{w}}{\partial \overline{z}^2}\right], \tag{2.3}$$

$$\overline{u}\frac{\partial \overline{w}}{\partial \overline{r}} + \overline{w}\frac{\partial \overline{w}}{\partial \overline{z}} = -\frac{1}{\rho}\frac{\partial \overline{p}}{\partial \overline{z}} + \nu\left[\frac{1}{\overline{r}}\frac{\partial}{\partial \overline{r}}\left(\overline{r}\,\frac{\partial \overline{w}}{\partial \overline{r}}\right) + \frac{\partial^2 \overline{w}}{\partial \overline{z}^2}\right]. \tag{2.4}$$

We define the following non-dimensional variables

$$u = \left(\frac{L}{\delta}\right)\frac{\overline{u}}{W_0}, \quad p = \frac{\overline{p} - p_\infty}{\rho W_0^2},$$

$$v = \frac{\overline{v}}{W_0}, \qquad r = \frac{\overline{r}}{\delta}, \tag{2.5}$$

$$w = \frac{\overline{w}}{W_0}, \qquad z = \frac{\overline{z}}{L},$$

where L is a characteristic scale in the z-direction, δ is a characteristic core radius, W_0 a characteristic axial flow velocity (e.g., free-stream velocity at the edge of the core), p_∞ the uniform static pressure far from the vortex, ρ the density, and ν the kinematic viscosity. In terms of these quantities the governing equations become

$$\frac{1}{r}\frac{\partial}{\partial r}(ru) + \frac{\partial w}{\partial z} = 0, \tag{2.6}$$

$$\left(\frac{\delta}{L}\right)^2\left[u\frac{\partial u}{\partial r} + w\frac{\partial u}{\partial z}\right] - \frac{v^2}{r} = -\frac{\partial p}{\partial r} + \frac{1}{Re_\delta}\left(\frac{\delta}{L}\right)\left[\frac{\partial}{\partial r}\left(\frac{1}{r}\frac{\partial}{\partial r}(ru) + \left(\frac{\delta}{L}\right)^2\frac{\partial^2 u}{\partial z^2}\right)\right], \tag{2.7}$$

$$u\frac{\partial v}{\partial r} + w\frac{\partial v}{\partial z} + \frac{uv}{r} = \frac{1}{Re_\delta}\left(\frac{L}{\delta}\right)\left[\frac{\partial}{\partial r}\left(\frac{1}{r}\frac{\partial}{\partial r}(rv)\right) + \left(\frac{\delta}{L}\right)^2\frac{\partial^2 v}{\partial z^2}\right], \tag{2.8}$$

$$u\frac{\partial w}{\partial r} + w\frac{\partial w}{\partial z} = -\frac{\partial p}{\partial z} + \frac{1}{Re_\delta}\left(\frac{L}{\delta}\right)\left[\frac{1}{r}\frac{\partial}{\partial r}(r\frac{\partial w}{\partial r}) + \left(\frac{\delta}{L}\right)^2\frac{\partial^2 w}{\partial z^2}\right], \tag{2.9}$$

where $Re_\delta \equiv W_0\delta/\nu$ is the Reynolds number based on the characteristic core radius.

Equations (2.6) - (2.9) contain two parameters: δ/L and Re_δ. At large distances upstream of breakdown the vortex develops on a length scale L which is much larger than δ, so $\delta/L \ll 1$ in this region. The core Reynolds numbers for which vortex breakdowns occur are large, but only modestly so, of the order of hundreds ([14-16], [18]). We see immediately that if $\delta/L \equiv \epsilon \ll 1$ that the axial viscous diffusion terms in the radial, azimuthal, and axial momentum equations, (2.7) - (2.9), are negligible compared to the other terms in these equations. If we take the formal limit $\epsilon \to 0$, with Re_δ held fixed, and without assuming that ϵRe_δ is either large or small, then (2.6) - (2.9) reduce to

$$\frac{1}{r}\frac{\partial}{\partial r}(ru) + \frac{\partial w}{\partial z} = 0, \tag{2.10}$$

$$-\frac{v^2}{r} = -\frac{\partial p}{\partial r}, \tag{2.11}$$

$$u\frac{\partial v}{\partial r} + w\frac{\partial v}{\partial z} + \frac{uv}{r} = \frac{1}{Re_\delta}\left(\frac{L}{\delta}\right)\left[\frac{\partial}{\partial r}\left(\frac{1}{r}\frac{\partial}{\partial r}(rv)\right)\right], \tag{2.12}$$

$$u\frac{\partial w}{\partial r}+w\frac{\partial w}{\partial z}=-\frac{\partial p}{\partial z}+\frac{1}{Re_\delta}\left(\frac{L}{\delta}\right)\left[\frac{1}{r}\frac{\partial}{\partial r}\left(r\frac{\partial w}{\partial r}\right)\right]. \tag{2.13}$$

Equations (2.10) - (2.13) are the so-called quasi-cylindrical equations, derived and extensively analyzed by Hall [3]. In contrast to Eqs. (2.6) - (2.9) which are elliptic, these quasi-cylindrical equations are parabolic equations, which can be solved by time-marching schemes. They differ from the ordinary boundary layer equations only by the inviscid radial momentum equation, (2.11), which contributes a non-zero normal pressure gradient. These equations were solved numerically by Hall [27] to predict the location of the onset of breakdown. Because upstream influence has been neglected they cannot be expected to predict the details of the breakdown itself.

As we approach breakdown the scale of z-derivatives becomes comparable to that of r-derivatives, so δ/L, even if small, is not expected to be infinitesimal. Hence, returning to Eqs. (2.6) - (2.9), for this near-breakdown region we again drop all terms of $O[(\delta/L)^2]$, but keep in addition to the $(L/\delta)Re_\delta^{-1}$ terms also terms of $O(\delta/L)$. (In other words, we are assuming that δ/L is small, but not infinitesimal, so terms of $O[(\delta/L)^2]$ may be neglected, but not those of $O(\delta/L)$.) There is only one such term in Eqs. (2.6) - (2.9), the second term on the right hand side of (2.7); this equation then becomes

$$-\frac{v^2}{r}=-\frac{\partial p}{\partial r}+\frac{1}{Re_\delta}\left(\frac{\delta}{L}\right)\frac{\partial}{\partial r}\left(\frac{1}{r}\frac{\partial}{\partial r}(ru)\right). \tag{2.14}$$

The other equations remain unchanged, viz. (2.10), (2.12) and (2.13). (Eq. (2.14) as a replacement for (2.11) in the near-breakdown region may be more formally justified by an appropriate rescaling of variables or by a multiple-scale argument.) In dimensional form the new set of reduced equations for the near-breakdown region is then

$$\frac{1}{r}\frac{\partial}{\partial r}(ru)+\frac{\partial w}{\partial z}=0, \tag{2.15}$$

$$u\frac{\partial u}{\partial r}+w\frac{\partial u}{\partial z}-\frac{v^2}{r}=-\frac{1}{\rho}\frac{\partial p}{\partial r}+\nu\frac{\partial}{\partial r}\left(\frac{1}{r}\frac{\partial}{\partial r}(ru)\right), \tag{2.16}$$

$$u\frac{\partial v}{\partial r}+w\frac{\partial v}{\partial z}+\frac{uv}{r}=\nu\frac{\partial}{\partial r}\left(\frac{1}{r}\frac{1}{\partial r}(rv)\right), \tag{2.17}$$

$$u\frac{\partial w}{\partial r}+w\frac{\partial w}{\partial z}=-\frac{1}{\rho}\frac{\partial p}{\partial z}+\frac{\nu}{r}\frac{\partial}{\partial r}\left(r\frac{\partial w}{\partial r}\right). \tag{2.18}$$

These equations differ from the full axisymmetric Navier-Stokes equations only by the omission of all the axial viscous diffusion terms and the inertia terms in the radial momentum equation. They differ from the quasi-cylindrical equations, (2.10) - (2.13), only by the inclusion of the radial viscous diffusion term in the radial momentum equation. Since, as for this

modified set of reduced equations, no axial viscous diffusion terms appear in (2.15) - (2.18) we would expect this set to be parabolic as well. As we shall see below, however, this is not so.

Combining (2.15) and (2.16) we can write

$$\frac{v^2}{r} = \frac{1}{\rho}\frac{\partial p}{\partial r} + \nu\frac{\partial^2 w}{\partial r \partial z}. \tag{2.19}$$

If we integrate this with respect to r from 0 to r, and then differentiate the resulting expression with respect to z, it becomes

$$\left(\frac{\partial p}{\partial z}\right)_{r=0} - \left(\frac{\partial p}{\partial z}\right)_{r} = -\rho\int_0^r \frac{1}{r}\frac{\partial v^2}{\partial z}dr + \mu\left[\frac{\partial^2 w}{\partial z^2}|_r - \frac{\partial^2 w}{\partial z^2}|_{r=0}\right]. \tag{2.20}$$

Multiplication of (2.17) by $2v$, and combining terms, leads to the expression

$$u\frac{\partial}{\partial r}(r^2v^2) + w\frac{\partial(r^2v^2)}{\partial z} = 2\nu r^2 v\frac{\partial}{\partial r}\left[\frac{1}{r}\frac{\partial}{\partial r}(rv)\right], \tag{2.21}$$

which can be used to eliminate $\partial v^2/\partial z$ in the integral term in (2.20), resulting in, dropping $|_r$,

$$\frac{\partial p}{\partial z}|_{r=0} - \frac{\partial p}{\partial z} = \rho\int_0^r \frac{1}{r^3}\left(\frac{u}{w}\right)\frac{\partial}{\partial r}(r^2v^2)dr - 2\mu\int_0^r \frac{1}{r}\left(\frac{v}{w}\right)\frac{\partial}{\partial r}\left[\frac{1}{r}\frac{\partial}{\partial r}(rv)\right]dr + \mu\left[\frac{\partial^2 w}{\partial z^2} - \frac{\partial^2 w}{\partial z^2}|_{r=0}\right]. \tag{2.22}$$

Equation (2.22) exhibits the various mechanisms that can lead to the development of an adverse pressure gradient along the core axis and consequent axial retardation of the flow. The first term on the right hand side is an inviscid term and was first identified in this context by Hall [3] from an inviscid analysis of the quasi-cylindrical equations. It is in the nature of a flow divergence-swirl interaction term, demonstrating how, for $u > 0$, arising from whatever cause, and positive $\partial k/\partial r$, where $k = rv$, which is generally the case, the pressure gradient along the axis can exceed that for larger r, and in particular that at the core edge. If Γ and R are characteristic measures of the core circulation (i.e., rv evaluated at the core edge) and radius, and we set $u/w = \alpha$, a measure of flow divergence, an order-of-magnitude analysis of this integral, evaluated at the core edge, yields (Hall [28])

$$\frac{\partial p}{\partial z}|_{r=0} - \frac{\partial p}{\partial z}|_{r=R} \sim \frac{\rho\alpha\Gamma^2}{R^3}. \tag{2.23}$$

Thus, if $\alpha > 0$, i.e. the stream surfaces diverge in the core, then the pressure gradient on the axis exceeds that along the core edge by an amount that can be very large for a concentrated, intense vortex core.

The two new terms on the right hand side of (2.22) are both viscous terms. The first of these, the second one on the right hand side, represents the interaction of swirl and radial

diffusion of swirl momentum, and also acts to raise the pressure on the axis. The last term on the right has the form of an axial diffusion term, which has arisen not from the inclusion of axial diffusion terms in the governing equations, because there are conspicuously absent from Eqs. (2.15) - (2.18), but from the continuity equation. Thus while the original quasi-cylindrical equations are parabolic, their modification, by the inclusion of the radial diffusion term in the radial momentum equation, has the effect of introducing a term which has the appearance of an axial diffusion term! This term gives an elliptic character to the equations. More precisely, (2.22) is an elliptic-integro-partial differential equation. In addition to showing how upstream influence enters the vortex breakdown problem, Eq. (2.22) also exhibits explicitly how flow divergence, $\alpha = u/w$, and the swirl ratio, v/w, independently affect the axial pressure gradient.

We can see more immediately the effect of the terms on the right hand side of (2.22) on the axial velocity by using (2.18) to eliminate $\partial p/\partial z$ from (2.22), obtaining

$$w\frac{\partial w}{\partial z}|_{r=0} - \nu\left[\frac{1}{r}\frac{\partial}{\partial r}\left(r\frac{\partial w}{\partial r}\right)\right]_{r=0} - \left(u\frac{\partial w}{\partial r} + w\frac{\partial w}{\partial z}\right)$$

$$+\frac{\nu}{r}\frac{\partial}{\partial r}\left(r\frac{\partial w}{\partial r}\right) = -\int_0^r \frac{1}{r^3}\left(\frac{u}{w}\right)\frac{\partial}{\partial r}(r^2v^2)dr \qquad (2.24)$$

$$+2\nu\int_0^r \frac{1}{r}\left(\frac{v}{w}\right)\frac{\partial}{\partial r}\left[\frac{1}{r}\frac{\partial}{\partial r}(rv)\right]dr - \nu\left[\frac{\partial^2 w}{\partial z^2} - \frac{\partial^2 w}{\partial z^2}|_{r=0}\right].$$

Equation (2.24) contains as unknowns the three velocity components. To complete the formulation of the problem we introduce the stream function ψ, defined such that

$$u = -\frac{1}{r}\frac{\partial \psi}{\partial z}, \quad w = \frac{1}{r}\frac{\partial \psi}{\partial r}, \qquad (2.25)$$

which makes the continuity equation automatically satisfied. Substitution of (2.25) into the azimuthal momentum equation, (2.17), results in

$$-\psi_z\frac{\partial v}{\partial r} - \psi_z v + \psi_r\frac{\partial v}{\partial z} = \nu r\frac{\partial}{\partial r}\left(\frac{1}{r}\frac{\partial}{\partial r}(rv)\right). \qquad (2.26)$$

Eliminating u and w in (2.24) using (2.25) yields

$$\psi_r\psi_{rz} - \psi_r\psi_{rz}|_{r=0} - r\psi_z\frac{\partial}{\partial r}\left(\frac{1}{r}\psi_r\right) - \nu r\left[\frac{\partial}{\partial r}\left(r\frac{\partial}{\partial r}\left(\frac{1}{r}\psi_r\right)\right) - \frac{\partial}{\partial r}\left(r\frac{\partial}{\partial r}\left(\frac{1}{r}\psi_r\right)\right)|_{r=0}\right]$$

$$= -r^2\int_0^r \frac{1}{r^3}\frac{\psi_z}{\psi_r}\frac{\partial}{\partial r}(r^2v^2)dr - 2\nu r^2\int_0^r \frac{v}{\psi_r}\frac{\partial}{\partial r}\left(\frac{1}{r}\frac{\partial}{\partial r}(rv)\right)dr + 2\nu r\left[\psi_{rzz} - \psi_{rzz}|_{r=0}\right]. \qquad (2.27)$$

Equations (2.26) and (2.27) are the governing equations for the unknowns ψ and v subject to appropriate boundary conditions. We note again that (2.27) is an elliptic-integro-partial differential equation.

3. Simplified Model

We noted earlier, in a discussion of expression (2.23), that if the flow divergence $\alpha = u/w > 0$, then it follows that $(\partial p/\partial z)_{r=0} > (\partial p/\partial z)_{r=R}$, i.e., flow divergence in such vortex flows can lead to a less favorable pressure gradient along the axis compared to that at the edge of the core. Equation (2.23) is based on a purely inviscid argument, nor is anything said about the origin of the streamline divergence. Within the inviscid assumption this may most readily be assumed to arise from an imposed adverse pressure gradient at the core edge, leading to axial flow retardation, and from continuity to $u > 0$. Could viscous effects either cause or alter the degree of axial retardation, independent of purely inviscid effects. Grabowski and Berger [14] conjectured that this could come about as follows. Viscous dissipation of swirl would lead to a decrease in v (Eq. (2.17)), so $\partial v/\partial z < 0$. It then follows from (2.11) that there will be greater adverse axial pressure gradient and axial velocity retardation near the axis than at the core edge. This, according to continuity, (2.15), will lead to a significant amount of outflow ($u > 0$). This outflow, in turn, because of conservation of angular momentum, will lead to a decrease in v (because r increases). The combination of outflow, and therefore flow divergence, and diffusion of swirl, leading to a decrease in v and hence making $\partial v/\partial z < 0$ will combine to make for a large adverse axial pressure gradient and resulting axial retardation near the axis. This picture of the flow closely parallels that of Hall [28].

The analysis presented in Section 2 attempts to capture this physics. The resulting formulation is, however, too complicated for the essentially new elements, those that distinguish this formulation from the quasi-cylindrical model, to be evident. In an attempt to illustrate these, we consider in this section a simplified version of the analysis of Section 2.

If we evaluate (2.24) at $r = R$, the edge of the core, noting that the viscous terms on the left hand side will be small there, as well as $u\,\partial w/\partial r$, $w\,\partial w/\partial z$, and $\partial^2 w/\partial z^2$, it reduces to

$$w\frac{\partial w}{\partial z}|_{r=0} = -\int_0^R \frac{1}{r^3}\left(\frac{u}{w}\right)\frac{\partial}{\partial r}(r^2v^2)dr + 2\nu\int_0^R \frac{1}{r}\left(\frac{v}{w}\right)\frac{\partial}{\partial r}\left[\frac{1}{r}\frac{\partial}{\partial r}(rv)\right]dr + \nu\frac{\partial^2 w}{\partial z^2}|_{r=0}. \quad (3.1)$$

We anticipate that in situations where breakdown occurs the sum of the two integrals on the right hand side of (3.1) is negative since this will lead to retardation on the axis ($\partial w/\partial z < 0$). Because these are integral terms they are less sensitive to the details of the velocity profiles, and as our greatest simplification we set the sum of these terms to a (negative) constant

$-A$, say. Equation (3.1) then becomes

$$\nu \frac{\partial^2 w}{\partial z^2}|_{r=0} - w \frac{\partial w}{\partial z}|_{r=0} \approx A, \quad (A > 0) \tag{3.2}$$

or, for simplicity

$$\nu \frac{d^2 w}{dz^2} - w \frac{dw}{dz} \equiv A, \tag{3.3}$$

where w in (3.3) is understood to be $w|_{r=0}$, the axial velocity on the axis.

First, we note that for small or negligible viscosity,

$$w \frac{dw}{dz} \approx -A, \tag{3.4}$$

with solution

$$\frac{1}{2} w^2 \approx -Az + \text{ const.}$$

If $w = W_c$ at $z = 0$, the uniform axial core velocity far upstream, then the const. in the above is $W_c^2/2$ and

$$w \approx W_c \left(1 - \frac{2A}{W_c^2} z\right)^{1/2}. \tag{3.5}$$

For small z this gives

$$w \approx W_c \left(1 - \frac{A}{W_c^2} z + \cdots\right), \tag{3.6}$$

a linear decrease of axial velocity on the axis. This is in qualitative and quantitative agreement with Hall's calculations [28] using the quasi-cylindrical equations.

3.1. Exact solution of non-linear model equation

Here we present the exact solution of non-linear Eq. (3.3). Integration yields immediately

$$\frac{dw}{dz} - \frac{1}{2\nu} w^2 = \left(\frac{A}{\nu}\right) z + a \quad (a = \text{const.}). \tag{3.7}$$

This is a Riccati equation. It can be transformed to a second-order linear ordinary differential equation by setting

$$w(z) = -2\nu \frac{y'(z)}{y(z)}. \tag{3.8}$$

Equation (3.7) becomes

$$\frac{d^2 y}{dz^2} + \frac{1}{2\nu} \left(\frac{A}{\nu} z + a\right) y = 0, \tag{3.9}$$

which is an Airy equation. It can be put in standard Airy equation form by introducing the new independent variable

$$\hat{z} = -\left(\frac{\nu}{2A^2}\right)^{1/3} \left(\frac{A}{\nu} z + a\right), \tag{3.10}$$

whereupon (3.9) becomes

$$\frac{d^2y}{d\hat{z}^2} - \hat{z}y = 0. \tag{3.11}$$

The general solution of (3.11) is

$$y(\hat{z}) = c_1 Ai(\hat{z}) + c_2 Bi(\hat{z}), \tag{3.12}$$

where c_1 and c_2 are arbitrary constants and Ai and Bi the Airy functions. In terms of the original dependent variable w the solution of (3.3) is then

$$w(\hat{z}) = (4A\nu)^{1/3}\frac{kAi'(\hat{z}) + Bi'(\hat{z})}{kAi(\hat{z}) + Bi(\hat{z})}, \tag{3.13}$$

where the arbitrary constants for the general solution of the second-order differential equation are a and k.

As boundary or initial conditions for (3.13) we have

$$\left.\begin{aligned} w &= W_c \\ \frac{dw}{dz} &= \left(\frac{dw}{dz}\right)_0, \text{ given} \end{aligned}\right\} \text{ at } z = 0. \tag{3.14a,b}$$

The first of these has already been discussed. As for the second, far upstream, at $z = 0$, the change in w with z may be small in the absence of an imposed pressure gradient, but this would not be so if this was not the case. Thus, for example, by choosing $(dw/dz)_0 < 0$ we can consider cases where an adverse pressure gradient, say as resulting from a diverging channel, is imposed at the core edge.

Applying first (3.14b) to (3.7), we find immediately

$$a = \left(\frac{dw}{dz}\right)_0 - \frac{1}{2\nu}W_c^2. \tag{3.15}$$

Since, when $z = 0$,

$$\hat{z} = -\left(\frac{\nu}{2A^2}\right)^{1/3} a = \hat{z}_0, \text{ say,} \tag{3.16}$$

so, applying boundary condition (3.14a)

$$W_c = (4A\nu)^{1/3}\frac{kAi'(\hat{z}_0) + Bi'(\hat{z}_0)}{kAi(\hat{z}_0) + Bi(\hat{z}_0)}. \tag{3.17}$$

Solving for k,

$$k = -\frac{W_c Bi(\hat{z}_0) - (4A\nu)^{1/3}Bi'(\hat{z}_0)}{W_c Ai(\hat{z}_0) - (4A\nu)^{1/3}Ai'(\hat{z}_0)}. \tag{3.18}$$

This completes the determination of the two constants a and k appearing in the general solution, (3.13), of the non-linear equation (3.3). The solution (3.13) depends on the four (dimensional) parameters A, ν, W_c, and $(dw/dz)_0$.

We note that if $(dw/dz)_0 = 0$, then

$$a = -\frac{1}{2\nu} W_c^2 \tag{3.19}$$

and the solution simplifies accordingly.

3.2. Asymptotic solution for $Re_\delta \to \infty$

We consider here, using matched asymptotic expansions, the asymptotic solution of the non-linear ordinary differential equation (3.3) for vanishingly small viscosity ν, i.e., in the limit $Re_\delta \to \infty$.

We begin with the outer expansion, which follows immediately from the first integral of (3.3), namely the expression (3.7), dropping, to lowest order, the first term on the left, so

$$\frac{1}{2} w^2 \sim -Az + \text{ const.} \tag{3.20}$$

If $w = W_c$ at $z = 0$, then the const. $= (1/2)W_c^2$, and the leading order outer solution is

$$w \sim W_c \left(1 - \frac{2A}{W_c^2} z\right)^{1/2}, \tag{3.21}$$

which is exactly the earlier (3.5).

To determine the scale of the inner variables, $\overline{z}$ and $\overline{w}$, we set

$$\begin{aligned} \overline{w} &= D\nu^\alpha w \qquad (\alpha < 0) \\ \overline{z} &= \left(\frac{W_c^2}{2A} - z\right) \nu^\beta \quad (\beta < 0) \end{aligned} \tag{3.22a, b}$$

where we anticipate both $\alpha, \beta < 0$. The differential equation (3.3) becomes

$$\nu^{2\beta-\alpha+1} \frac{d^2\overline{w}}{d\overline{z}^2} - D^{-1}\nu^{-2\alpha+\beta} \overline{w} \frac{d\overline{w}}{d\overline{z}} = AD. \tag{3.23}$$

The two terms on the left hand side will be of the same order in ν if

$$\beta + \alpha = -1.$$

If we choose α and β such that the single term on the right hand side vanishes in the limit as $\nu \to 0$, then the resulting inner solution cannot be matched with the outer solution. Therefore we must choose

$$-2\alpha + \beta = 0, \quad \text{or } \beta = 2\alpha.$$

It then follows that

$$\alpha = -1/3, \quad \beta = -2/3. \tag{3.24}$$

Thus the scaling of the inner variables is

$$\begin{aligned} \overline{w} &= \frac{Dw}{\nu^{1/2}}, \qquad\qquad \text{or} \quad w = D^{-1}\nu^{1/3}\overline{w} \\ \overline{z} &= \left(\frac{W_c^2}{2A} - z\right)\nu^{-2/3}, \quad \text{or} \quad z = \frac{W_c^2}{2A} - \overline{z}\nu^{2/3}. \end{aligned} \tag{3.25}$$

Equation (3.23) becomes

$$\frac{d^2\overline{w}}{d\overline{z}^2} + D^{-1}\overline{w}\frac{d\overline{w}}{d\overline{z}} = AD. \tag{3.26}$$

This equation for the inner region is identical, apart from a change of variables, with the full equation, (3.3). The following analysis therefore proceeds along the lines of that given in Section 3.1.

The first integral of (3.26) is

$$\frac{d\overline{w}}{d\overline{z}} + \frac{1}{2D}\overline{w}^2 = AD\overline{z} + a, \quad (a = \text{const.}) \tag{3.27}$$

This Ricatti equation can be converted to a second order linear equation by the substitution $\overline{w} \propto y'/y$. The solution of the resulting Airy equation is

$$\overline{w}(\hat{z}) \sim (4A)^{1/3} D \frac{kAi'(\hat{z}) + Bi'(\hat{z})}{kAi(\hat{z}) + Bi(\hat{z})}, \tag{3.28a}$$

where

$$\hat{z} = \frac{(2A^2)^{-1/3}}{D}(AD\overline{z} + a), \tag{3.28b}$$

a and k being arbitrary constants, to be determined by matching of the inner and outer solutions.

To match the outer solution (3.21) and the inner solution (3.28), we begin by rewriting the outer solution (3.21) in inner variables and expanding for $\nu \to 0$, with $\overline{z}$ held fixed, obtaining

$$w_{\text{outer}}^2 \sim 2A\overline{z}\nu^{2/3}. \tag{3.29}$$

Rewritten in outer variables the inner variable $\hat{z}$ is

$$\hat{z} = \frac{A^{-2/3}}{2^{1/3}D}\left[AD\left(\frac{W_c^2}{2A} - z\right)\nu^{-2/3} + a\right]. \tag{3.30}$$

For reasons discussed earlier $A > 0$, and we can assume that D, a scale factor for $\overline{w}$, is also positive. It then follows that in the limit $\nu \to 0$, with z held fixed, that

$$\begin{aligned} \hat{z} &\to \infty \text{ if } \frac{W_c^2}{2A} - z > 0, \\ \hat{z} &\to -\infty \text{ if } \frac{W_c^2}{2A} - z < 0. \end{aligned} \tag{3.31}$$

If the second of these alternatives is the case, $Ai(\hat{z})$ and $Bi(\hat{z})$ oscillate and the inner solution (3.28) cannot be matched to the outer solution, (3.29). Therefore we assume the first case, that $\hat{z} \to \infty$ as $\nu \to 0$. For asymptotically large positive arguments Ai and Bi have the following asymptotic expansions

$$\text{as } \hat{z} \to \infty \begin{cases} Ai(\hat{z}) \sim \dfrac{1}{2\sqrt{\pi}} \hat{z}^{-1/4} e^{-2\hat{z}^{3/2}/3}, \\ Ai'(\hat{z}) \sim \dfrac{-1}{2\sqrt{\pi}} \hat{z}^{1/4} e^{-2\hat{z}^{3/2}/3}, \end{cases} \quad \begin{cases} Bi(\hat{z}) \sim \dfrac{1}{\sqrt{\pi}} \hat{z}^{-1/4} e^{2\hat{z}^{3/2}/3}, \\ Bi'(\hat{z}) \sim \dfrac{1}{\sqrt{\pi}} \hat{z}^{1/4} e^{2\hat{z}^{3/2}/3}. \end{cases} \tag{3.32}$$

It then follows that in this (outer) limit that (3.28a) behaves asymptotically as

$$\overline{w}(\hat{z}) \sim (4A)^{1/3} D \hat{z}^{1/2}, \tag{3.33}$$

so, according to (3.25) and (3.28b),

$$\begin{aligned} w_{\text{inner}} &\sim (4A)^{1/3} \nu^{1/3} \hat{z}^{1/2} \\ &\sim (4A)^{1/3} \nu^{1/3} \left[\frac{(2A)^{-1/3}}{D} (AD\overline{z} + a) \right]^{1/2} \end{aligned}$$

or,

$$w_{\text{inner}}^2 \sim \left(2A\overline{z} + \frac{2a}{D} \right) \nu^{2/3}. \tag{3.34}$$

The variable part of the inner and outer solutions, (3.29) and (3.34) agree exactly.

3.3. Exact solution in the limit of vanishingly small viscosity

We consider the limit of the exact solution given in Section 3.1 as $\nu \to 0$. In this limit, from (3.15) and (3.16),

$$a \to -\frac{1}{2\nu} W_c^2 \to \infty, \tag{3.35a}$$

$$\hat{z}_0 = -\left(\frac{\nu}{2A^2} \right)^{1/3} a \to -\left(\frac{\nu}{2A^2} \right)^{1/3} \left(-\frac{1}{2\nu} W_c^2 \right) \to +\infty, \tag{3.35b}$$

From (3.18), using the asymptotic expressions (3.32),

$$\lim_{\nu \to 0} k = 0. \tag{3.35c}$$

From (3.10)

$$\begin{aligned} \lim_{\nu \to 0} \hat{z} &\rightarrow -\left(\frac{\nu}{2A^2}\right)^{1/3} \left(\frac{A}{\nu} z - \frac{1}{2\nu} W_c^2\right) \\ &\rightarrow \frac{1}{2}(2A^2\nu^2)^{-1/3}(W_c^2 - 2Az) \end{aligned} \tag{3.36a}$$

$$\rightarrow \begin{cases} +\infty, \text{ if } W_c^2 > 2Az \\ -\infty, \text{ if } W_c^2 < 2Az. \end{cases} \tag{3.36b}$$

We assume that $W_c^2 > 2Az$, so $\hat{z} \rightarrow +\infty$ as $\nu \rightarrow 0$. It then follows from (3.13), using (3.35c), (3.32) and (3.36a), that

$$\begin{aligned} \lim_{\nu \to 0} w(\hat{z}) &\rightarrow (4A\nu)^{1/3}\hat{z}^{1/2} = (4A\nu)^{1/3}\left[\frac{1}{2}(2A^2\nu^2)^{-1/3}\left(W_c^2 - 2Az\right)\right]^{1/2}, \\ &\rightarrow (W_c^2 - 2Az)^{1/2}, \end{aligned} \tag{3.37}$$

which is identical with the outer solution, (3.21), presented in Section 3.2 as part of the asymptotic solution for $Re_\delta \rightarrow \infty$, and with the limiting small viscosity solution given earlier (Eq. 3.5).

3.4. Non-dimensionalization

We begin our non-dimensionalization of (3.3) by first considering the quantity on the right hand side, A, which stands for the (negative of the) two integral terms on the right hand side of (3.1). We consider each of these in turn. The order of magnitude of the first of these can be estimated as follows:

$$-\int_0^R \frac{1}{r^3}\left(\frac{u}{w}\right)\frac{\partial}{\partial r}(r^2v^2)dr \sim -\left(\frac{\alpha}{\delta^3}\right)\left(\frac{\Gamma^2}{\delta}\right)\delta = -\left(\frac{\alpha}{\delta^3}\right)\Gamma^2, \tag{3.38}$$

where $rv = k \sim \Gamma$, the characteristic circulation of the vortex, δ the characteristic core radius ($\sim R$), and $u/w \sim \alpha$, a characteristic flow divergence.

The magnitude of the second integral on the right hand side of (3.1) is similarly estimated:

$$2\nu\int_0^R \frac{1}{r}\left(\frac{v}{w}\right)\frac{\partial}{\partial r}\left[\frac{1}{r}\frac{\partial}{\partial r}(rv)\right]dr \sim 2\nu\left(\frac{s}{\delta^2}\right)\left(\frac{\Gamma}{\delta^2}\right)\delta = 2\nu\left(\frac{s}{\delta^3}\right)\Gamma, \tag{3.39}$$

where $v/w \sim s$, a characteristic swirl velocity ratio. (Both integrals have dimensions of LT^{-2}.) Unlike (3.38) which is generally negative as the vortex approaches breakdown, the

sign of the second integral is not obvious. To allow us to consider the effect of the integral being negative (driving the vortex to breakdown) or positive, we shall attach to it an arbitrary sign, denoted by *sgn*. Then

$$A \sim \frac{\alpha}{\delta^3}\Gamma^2 + 2\ \mathrm{sgn}\nu\left(\frac{s}{\delta^3}\right)\Gamma, \tag{3.40}$$

and the differential equation (3.3) becomes

$$\nu\frac{d^2w}{dz^2} - w\frac{dw}{dz} = \left(\frac{\alpha}{\delta^3}\right)\Gamma^2 + 2\ \mathrm{sgn}\ \nu\left(\frac{s}{\delta^3}\right)\Gamma. \tag{3.41}$$

We now non-dimensionalize (3.41) by defining non-dimensional variables and parameters

$$\begin{aligned} \overline{z} &= \frac{z}{\delta}, \quad \overline{w} = \frac{w}{W_c}, \\ \gamma &= \frac{\Gamma}{\delta W_c}, \quad Re_\delta = \frac{W_c\delta}{\nu}, \end{aligned} \tag{3.42}$$

with which definitions (3.41) becomes

$$\frac{1}{Re_\delta}\frac{d^2\overline{w}}{d\overline{z}^2} - \overline{w}\frac{d\overline{w}}{d\overline{z}} = \alpha\gamma^2 + \frac{2}{Re_\delta}\ \mathrm{sgn}s\gamma. \tag{3.43}$$

The solution of (3.43) depends on the four parameters Re_δ, the core Reynolds number, $\alpha(\sim u/w)$, the flow divergence, $s(\sim v/w)$, the swirl velocity ratio, and $\gamma(= \Gamma/\delta W_c)$, the non-dimensional flow circulation.

4. Calculations and Results

We have calculated a number of solutions of Eq. (3.43), by evaluation of the exact solution given in Section 3.1, in order to exhibit the dependence of the solutions on the four parameters Re_δ, α, s, and γ which appear in the equation, and the value of the initial velocity gradient $(dw/dz)_0$. Figures 1 and 2 show the non-dimensional axial velocity variation $w(z)$ with Re_δ (for convenience the bars over the non-dimensional variables introduced in Section 3.4 have been removed) for the same values of $(dw/dz)_0(= -0.1)$ and $\alpha(= 0.005)$ but different values of $s(= 0.5$ and $1.0)$ and $\gamma(= 1.0$ and $1.5)$. (We anticipate that negative values of $(dw/dz)_0$, corresponding to an adverse axial pressure gradient, are most likely to lead to breakdown; this is borne out by sample calculations of such cases. Also, in all the calculations reported here the *sgn* in (3.40) is taken to be positive, implying that the integral in (3.39) is negative, as is that in (3.38), increasing the tendency of the vortex to undergo breakdown.) We note that for both cases in Figs. 1 and 2 the vortex undergoes breakdown, i.e., the axial velocity becomes zero, for all Re_δ in the range $50 \leq Re_\delta \leq 1000$, except

possibly for $Re_\delta = 1000$. Moreover, the point on the axis where stagnation or breakdown occurs moves rapidly upstream as Re_δ increases, reaching asymptotically a position close to the initial station. Finally we note that the curves in Figs. 1 and 2 are remarkably similar for the same Re_δ, suggesting that the results are insensitive to the values of s and γ. Calculations confirm this for other values of the parameters as well. Figure 3 shows the axial velocity for the same Re_δ range and the same s and γ as in Fig. 2 but a smaller value of α and a larger negative initial axial velocity gradient. We note in comparing Fig. 3 to 2 the much more rapid decrease in axial velocity as Re_δ increases. This is primarily a consequence of the much larger negative value of $(dw/dz)_0$ in Fig. 3. (That the change in α has only a small effect can be seen, for example, from Fig. 4 for the same values of all the parameters as in Fig. 3 except for α which is ten times as large, 0.01 as compared to 0.001. There is very little discernible difference between the curves in Figs. 3 and 4.) Figure 5 shows the same curves for the same values of the parameters as in Fig. 2 except that for Fig. 5 $|(dw/dz)_0|$ is a tenth as large. The consequence of this is that compared to Fig. 2 the curves are displaced further downstream, and even more significantly, for the smaller Re_δ the axial flow does not stagnate but remains relatively constant and then increases with axial distance! Again this illustrates the importance of the value of the initial axial velocity gradient.

Because of the particular significance of the value of the axial location where the axial velocity becomes zero, denoting the location of breakdown, we have used the method of continuation [29] to determine the variation of this point as a function of the various parameters. The results above, as well as others unreported here, demonstrate that the point at which the axial velocity becomes zero, denoted by $z_{v.b.}$, varies primarily with the parameters Re_δ and $(dw/dz)_0$. Figure 6 shows the variation of $z_{v.b.}$ with Re_δ for four values of $-(dw/dz)_0$; the other parameters have the values $\alpha = 0.01$, $\gamma = 1$, and $s = 0.5$. We see that for all these values of the initial gradient the location of axial stagnation moves rapidly upstream, and that while the exact values of $z_{v.b.}$ asymptote for larger Re_δ there are significant differences for smaller Re_δ. Figure 7 shows, for $Re = 500$, $\alpha = 0.015$, $\gamma = 1$, and $s = 0.5$, the variation of $z_{v.b.}$ with $-(dw/dz)_0$. We note the very rapid upstream migration of the location of axial breakdown as the initial axial velocity gradient becomes more negative, i.e., larger initial adverse pressure gradient.

5. Conclusions

The principal aims of this paper were to show the origin of the pronounced tendency of the location of vortex breakdown to migrate upstream, an effect characteristic of most numerical simulations and noted in some experiments. Based on an order-of-magnitude analysis of the viscous Navier-Stokes equations a modified set of governing differential equations for swirling

flows has been derived. A theoretical analysis of these equations shows that unlike the parabolic quasi-cylindrical equations, which they resemble, these equations have an elliptic character. This analysis also exhibits how the location of axial stagnation, interpreted here as a signal of breakdown, depends explicitly on a number of parameters: the core Reynolds number, the flow divergence, the swirl velocity ratio, and the strength of the vortex. A simplified model for the axial velocity variation is presented and solved exactly. Numerical results obtained from this solution for a range of the governing parameters show that there is a very pronounced tendency of the breakdown location to move upstream as the core Reynolds number increases, or the initial adverse pressure gradient increases, in qualitative accord with most numerical and experimental simulations.

References

[1] Berger, S. A., 1992. "Ellipticity in the vortex breakdown problem," Instability, Transition and Turbulence (Eds. M. Y. Hussaini, A. Kumar, and C. L. Streett), Springer-Verlag, NY, pp. 96-106.

[2] Hall, M. G., 1965. "A numerical method for solving the equations for a vortex core," *Aero Res. Council* R&M 3467, 29 pp.

[3] Hall, M. G., 1966. "The structure of concentrated vortex cores," *Prog. Aero. Sci.* **7**, pp. 53-110.

[4] Mager, A., 1972. "Dissipation and breakdown of a wing-tip vortex," *J. Fluid Mech.* **55**, pp. 609-28.

[5] Ludwieg, H., 1962. "Zur Erklarung der Instabilitat der uber angestellten Deltaflugeln auftretenden freien Wirbelkerne," *Z. Flugwiss.* **10**, pp. 242-49.

[6] Ludwieg, H., 1965. "Erklarung des Wirbelaufplatzens mit Hilfe der Stabilitatstheorie fur Stromungen mit schraubenlinienformigen Stromlinien," *Z. Flugwiss* **13**, pp. 437-42.

[7] Squire, H. B., 1960. "Analysis of the "vortex breakdown" phenomenon. Part 1," Aero. Dept., Imperial Coll., London, Rep. 102. Also in *Miszellaneen der Angewandten Mechanik*, pp. 306-12, Akademie-Verlag, Berlin.

[8] Benjamin, T. B., 1962. "Theory of the vortex breakdown phenomenon," *J. Fluid Mech.* **14**, pp. 593-629.

[9] Benjamin, T. B., 1967. "Some developments in the theory of vortex breakdown," *J. Fluid Mech.* **28**, pp. 65-84.

[10] Leibovich, S., 1970. "Weakly non-linear waves in rotating fluids," *J. Fluid Mech.* **42**, pp. 803-822.

[11] Randall, J. D. and Leibovich, S., 1973. "The critical state: A trapped wave model of vortex breakdown," *J. Fluid Mech.* **58**, pp. 495-515.

[12] Spall, R. E., Gatski, T. B., and Grosch, C. E., 1987. "A criterion for vortex breakdown," *Phys. Fluids* **30**, pp. 3434-3440.

[13] Kopecky, R. M. and Torrance, K. E., 1973. "Initiation and structure of axisymmetric eddies in a rotating stream," *Comput. Fluids* **1**, pp. 289-300.

[14] Grabowski, W. J. and Berger, S. A., 1976. "Solutions of the Navier-Stokes equations for vortex breakdown," *J. Fluid Mech.* **75**, pp. 525-544.

[15] Hafez, M., Kuruvila, G., and Salas, M. D., 1986. "Numerical study of vortex breakdown," *Appl. Numer. Math.* **2**, pp. 291-302.

[16] Salas, M. D. and Kuruvila, G., 1989. "Vortex breakdown simulation: A circumspect study of the steady, laminar, axisymmetric model," *Comput. Fluids* **17**, pp. 247-262.

[17] Kuruvila, G. and Salas, M. D., 1990. "Three-dimensional simulation of vortex breakdown," NASA Tech. Mem. 102664.

[18] Spall, R. E., Gatski, T. B., and Ash, R. L., 1990. "The structure and dynamics of bubble-type vortex breakdown," *Proc. Roy. Soc. Lond. A* **429**, pp. 613-637.

[19] Spall, R. E. and Gatski, T. B., 1991. "A computational study of the topology of vortex breakdown," *Proc. Roy. Soc. Lond. A* **435**, pp. 321-337.

[20] Breuer, M. and Hanel, D., 1989. "Solution of the 3-D, incompressible Navier-Stokes equations for the simulation of vortex breakdown," 8th GAMM Conf., Delft. Notes on Numerical Fluid Dynamics, Vieweg Verlag.

[21] Menne, S. and Liu, C. H., 1990. "Numerical simulation of a three-dimensional vortex breakdown," *Z. Flugwiss. Weltraumforsch.* **14**, pp. 301-308.

[22] Lugt, H. J. and Haussling, H. J., 1982. "Axisymmetric vortex breakdown in rotating fluid within a container," *Trans. ASME E: J. Appl. Mech.* **49**, pp. 921-923.

[23] Lugt, H. J. and Abboud, M., 1987. "Axisymmetric vortex breakdown with and without temperature effects in a container with a rotating lid," *J. Fluid Mech.* **179**, pp. 179-200.

[24] Neitzel, G. P., 1988. "Streak-line motion during steady and unsteady axisymmetric vortex breakdown," *Phys. Fluids* **31**, pp. 958-960.

[25] Bar-Yoseph, P., Seelig, S., Solan, A., and Roesner, K. G., 1987. "Vortex breakdown in spherical gap," *Phys. Fluids* **30**, pp. 1581-83.

[26] Escudier, M. P., 1984. "Observations of the flow produced in a cylindrical container by a rotating endwall," *Expts. Fluids* **2**, pp. 189-196.

[27] Leibovich, S., 1978. "The structure of vortex breakdown," *Ann. Rev. Fluid Mech.* **10**, pp. 221-46.

[28] Hall, M. G., 1972. "Vortex breakdown," *Ann. Rev. Fluid Mech.* **4**, pp. 195-218.

[29] Keller, H. B., 1987. *Lectures on Numerical Methods in Bifurcation Problems*, Springer-Verlag, NY.

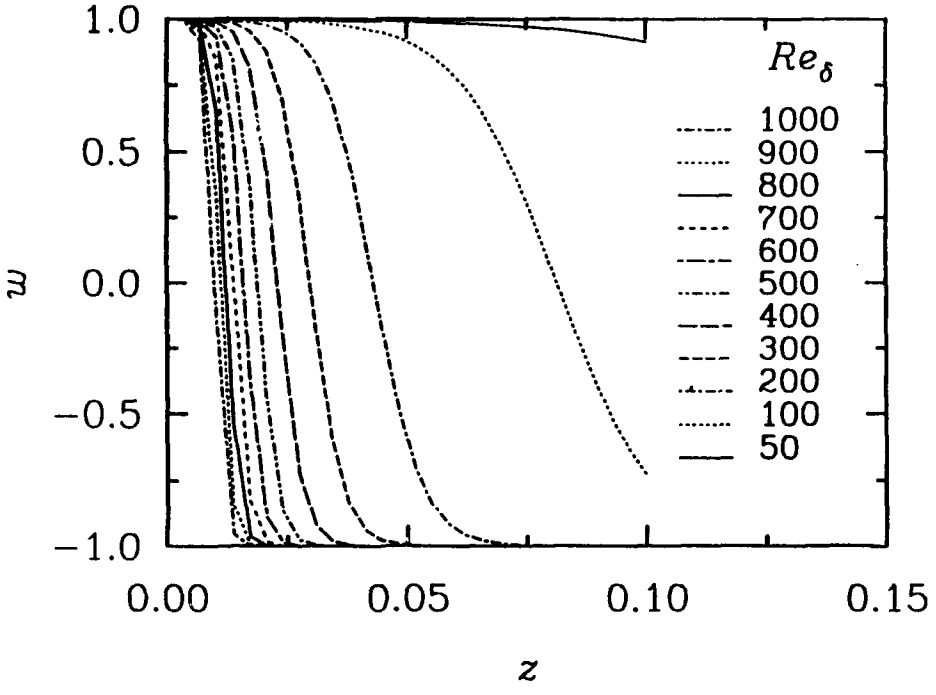

Figure 1. Variation of axial velocity with axial distance for different core Reynolds numbers; parameters: $\alpha = 0.005$, $\gamma = 1.5$, $s = 1.0$; initial axial velocity gradient, $(\partial w/\partial z)_0 = -0.1$.

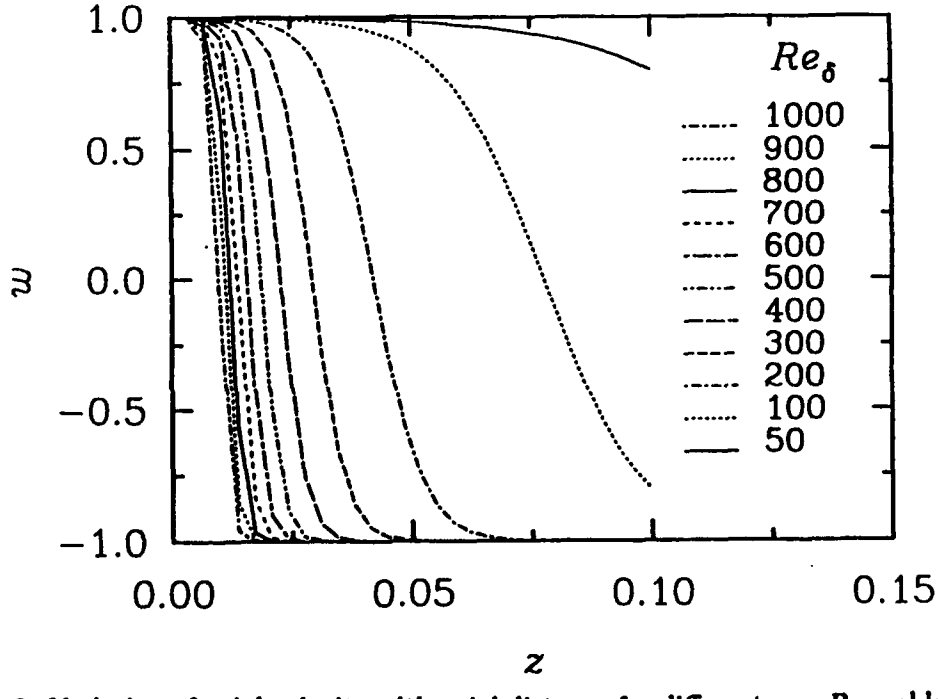

Figure 2. Variation of axial velocity with axial distance for different core Reynolds numbers; parameters: $\alpha = 0.005$, $\gamma = 1$, $s = 0.5$; initial axial velocity gradient, $(\partial w/\partial z)_0 = -0.1$.

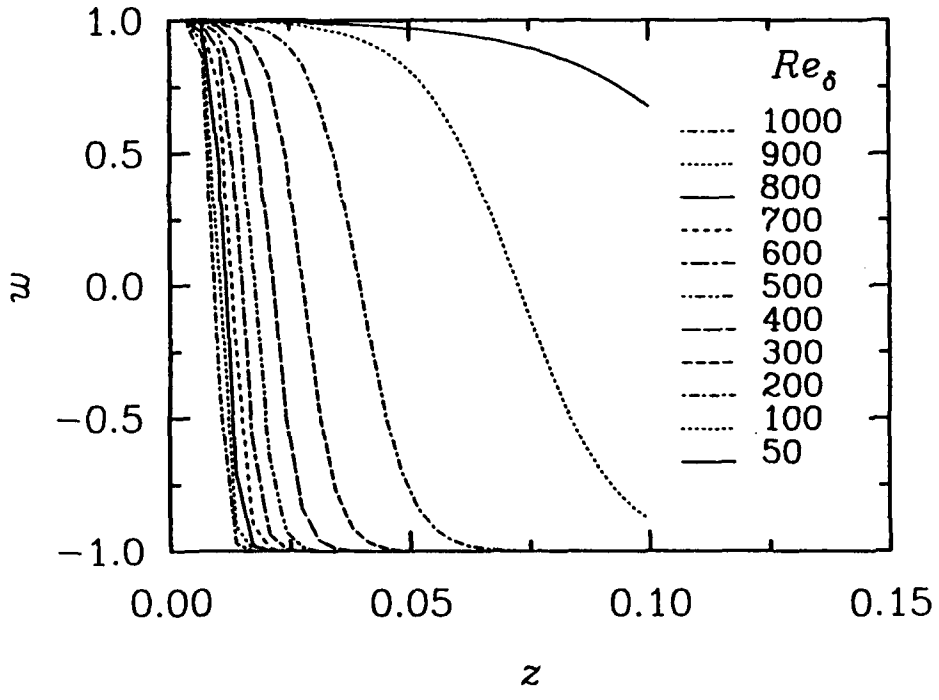

Figure 3. Variation of axial velocity with axial distance for different core Reynolds numbers; parameters: $\alpha = 0.001$, $\gamma = 1$, $s = 0.5$; initial axial velocity gradient, $(\partial w/\partial z)_0 = -0.15$.

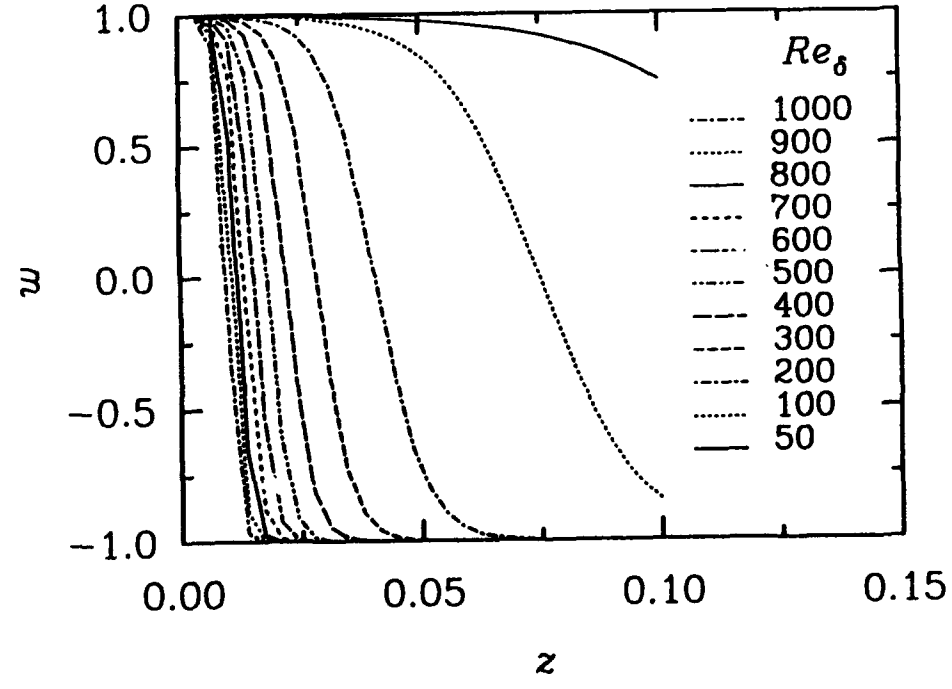

Figure 4. Variation of axial velocity with axial distance for different core Reynolds numbers; parameters: $\alpha = 0.01$, $\gamma = 1$, $s = 0.5$; initial axial velocity gradient, $(\partial w/\partial z)_0 = -0.15$.

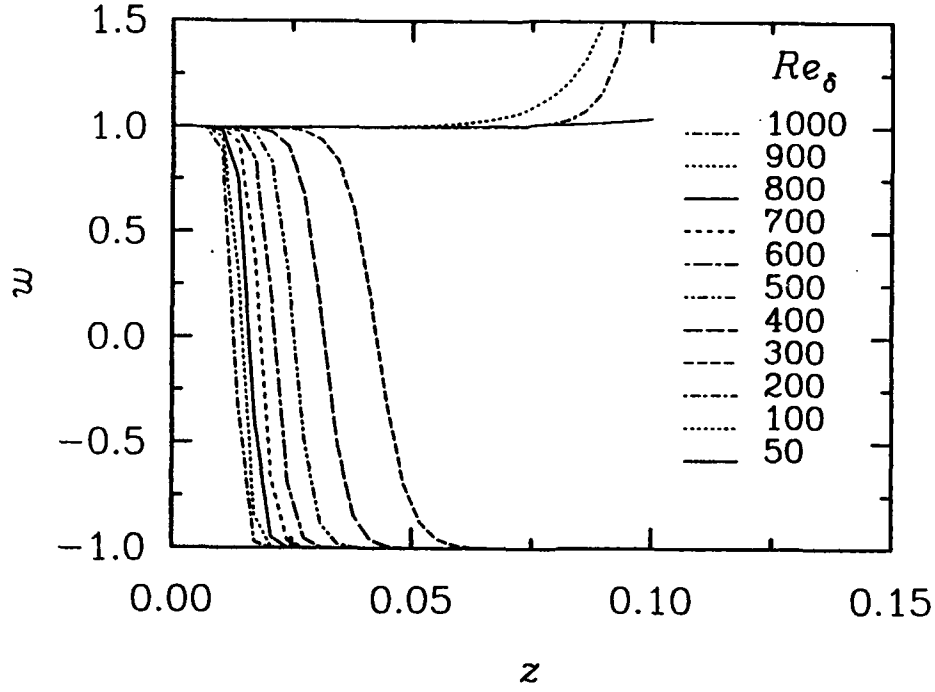

Figure 5. Variation of axial velocity with axial distance for different core Reynolds numbers; parameters: $\alpha = 0.005$, $\gamma = 1$, $s = 0.5$; initial axial velocity gradient, $(\partial w/\partial z)_0 = -0.01$.

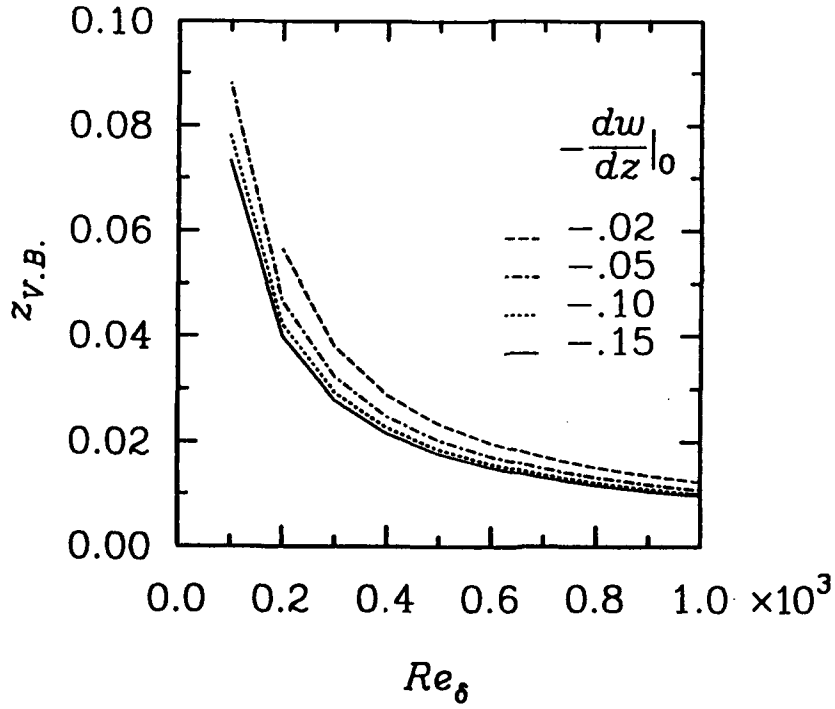

Figure 6. Location of the axial vortex breakdown point as a function of core Reynolds number for different initial axial velocity gradients; parameters: $\alpha = 0.01$, $\gamma = 1$, $s = 0.5$.

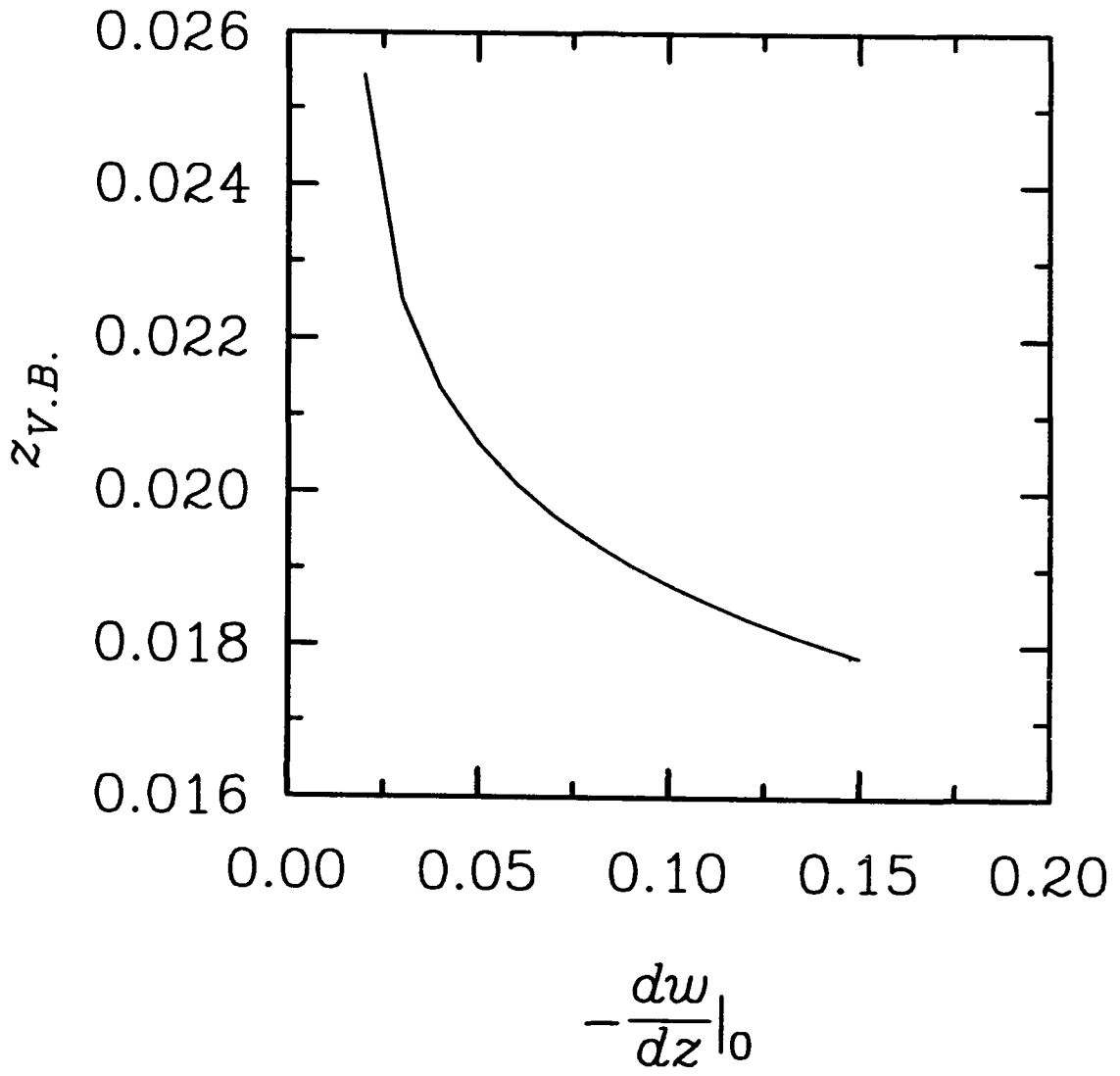

Figure 7. Location of the axial vortex breakdown point as a function of the initial (negative) axial velocity gradient; parameters: $\alpha = 0.015$, $\gamma = 1$, $s = 0.5$, $Re_\delta = 500$.

REPORT DOCUMENTATION PAGE

Form Approved
OMB No. 0704-0188

[illegible]

1. AGENCY USE ONLY (Leave blank)	2. REPORT DATE November 1992	3. REPORT TYPE AND DATES COVERED Contractor Report
4. TITLE AND SUBTITLE VORTEX BREAKDOWN INCIPIENCE: THEORETICAL CONSIDERATIONS		5. FUNDING NUMBERS C NAS1-18605 C NAS1-19480 WU 505-90-52-01
6. AUTHOR(S) Stanley A. Berger Gordon Erlebacher		
7. PERFORMING ORGANIZATION NAME(S) AND ADDRESS(ES) Institute for Computer Applications in Science and Engineering Mail Stop 132C, NASA Langley Research Center Hampton, VA 23681-0001		8. PERFORMING ORGANIZATION REPORT NUMBER ICASE Report No. 92-63
9. SPONSORING/MONITORING AGENCY NAME(S) AND ADDRESS(ES) National Aeronautics and Space Administration Langley Research Center Hampton, VA 23681-0001		10. SPONSORING/MONITORING AGENCY REPORT NUMBER NASA CR-189734 ICASE Report No. 92-63
11. SUPPLEMENTARY NOTES Langley Technical Monitor: Michael F. Card Final Report		To be submitted to Theoretical and Computational Fluid Dynamics
12a. DISTRIBUTION/AVAILABILITY STATEMENT Unclassified - Unlimited Subject Category 02, 34		12b. DISTRIBUTION CODE

13. ABSTRACT (Maximum 200 words)

The sensitivity of the onset and the location of vortex breakdowns in concentrated vortex cores, and the pronounced tendency of the breakdowns to migrate upstream have been characteristic observations of experimental investigations; they have also been features of numerical simulations and led to questions about the validity of these simulations. This behavior seems to be inconsistent with the strong time-like axial evolution of the flow, as expressed explicitly, for example, by the quasi-cylindrical approximate equations for this flow. An order-of-magnitude analysis of the equations of motion near breakdown leads to a modified set of governing equations, analysis of which demonstrates that the interplay between radial inertial, pressure, and viscous forces gives an elliptic character to these concentrated swirling flows. Analytical, asymptotic, and numerical solutions of a simplified non-linear equation are presented; these qualitatively exhibit the features of vortex onset and location noted above.

14. SUBJECT TERMS vortex breakdown			15. NUMBER OF PAGES 26
			16. PRICE CODE A03
17. SECURITY CLASSIFICATION OF REPORT Unclassified	18. SECURITY CLASSIFICATION OF THIS PAGE Unclassified	19. SECURITY CLASSIFICATION OF ABSTRACT	20. LIMITATION OF ABSTRACT